

Optical scattering resonances of single plasmonic nanoantennas

O. L. Muskens* and J. Gómez Rivas

*FOM Institute for Atomic and Molecular Physics AMOLF, c/o Philips Research Laboratories,
High Tech Campus 4, 5656 AE, Eindhoven, The Netherlands*

V. Giannini and J. A. Sánchez-Gil

Instituto de Estructura de la Materia, Consejo Superior de Investigaciones Científicas, Serrano 121, 28006 Madrid, Spain

(Dated: March 23, 2022)

We investigate the far-field optical resonances of individual dimer nanoantennas using confocal scattering spectroscopy. Experiments on a single-antenna array with varying arm lengths and interparticle gap sizes show large spectral shifts of the plasmon modes due to a combination of geometrical resonances and plasmon hybridization. All resonances are considerably broadened compared to those of small nanorods in the quasistatic limit, which we attribute to a greatly enhanced radiative damping of the antenna modes. The scattering spectra are compared with rigorous model calculations that demonstrate both the near-field and far-field characteristics of a half-wave antenna.

PACS numbers: 78.67.bf, 42.25.Fx, 73.20.mf

The optical resonances of small noble metal particles have been under investigation for many years.¹ Their optical properties are governed by quasistatic oscillations of free electrons, resulting in a surface plasmon resonance. Small metal particles hold promise for applications in bio-labeling² and optical sensing.³ On the other hand, surface plasmon polaritons on metal films are receiving attention for applications in optical data communication.⁴ Between the limits of a small particle and a planar film, a surprisingly rich playground exists of complex plasmonic structures supporting either localized or propagating surface plasmon resonances, or a combination of both.⁵ The mode spectrum of these complex plasmonic structures and their coupling to the radiation field is a topic of intensive theoretical and experimental studies.⁶

The regime of polariton-like modes has been investigated for elongated rods supporting higher order longitudinal resonances in the visible and near-infrared.^{7,8,9,10,11} Nodes and antinodes were found in the plasmonic mode structure that correspond to multiples of half the surface plasmon polariton wavelength. The modes were shown to constitute a dispersion relation for the surface plasmon polaritons in the nanorod resonator.^{8,9,10} Due to their analogy with traditional radiowave antennas as convertor of electrical current to radiation, surface plasmon polariton resonators have recently been referred to as optical antennas.^{12,13} By coupling two resonant structures to form a dimer, it was shown that nonlinear optical phenomena can be greatly enhanced.^{12,13,14} Which antenna design is the most suitable for specific applications, like field enhancement^{12,13} or light extraction^{14,15}, is a question of considerable importance.

Here, we present the first simultaneous study of the effects of particle length and gap width on the far-field resonances of dimer nanoantennas. By performing single-particle spectroscopy, we gain access to the homogeneous spectral width of the antenna modes. We find fundamental differences between the purely geometrical resonances of nanoantennas^{11,12} and the quasistatic material-

dependent resonances of small ellipsoidal particles, used for many years in the description of chemically prepared nanorods.¹⁶ A strong increase of the radiative damping of antennas is found with respect to small nanorods in the quasistatic limit¹⁷, which we discuss in the context of nanoantenna design for various applications. We corroborate our experimental results using rigorous model calculations that are exact from the electrodynamic point of view, i.e. free from dipolar and/or non-retarded approximations. These model calculations clearly demonstrate both the near-field and far-field characteristics of a half-wave antenna mode.

Individual nanoantennas are fabricated using high-resolution electron-beam lithography, producing gold nanostructures of 20-nm thickness. The substrate is a silicon wafer covered by a 500-nm layer of thermally grown silica. SEM-images of an array of nanoantennas are shown in Fig. 1(a), together with detailed images of several individual nanorods and antenna structures. In the array, the antenna arm length, L , is varied in the vertical direction, while the antenna gap width, Δ , is varied in the horizontal direction. For additional experiments described in another paper¹⁸, the structures were covered with a 10 nm thin layer of silica and a 10 nm polymer film. Together with the silica substrate, this results in a nearly homogeneous embedding of the antennas in a medium with a dielectric constant ϵ_m of ~ 1.5 .

The plasmonic modes of individual antennas are characterized by scattering spectroscopy using a darkfield microscope equipped with confocal detection. The illumination geometry consists of a cone of grazing-incidence wavevectors defined by the ~ 0.95 NA illumination ring. Scattered photons are collected by a $100\times$, 0.9 N.A. objective and detected, after confocal filtering, by an avalanche photodiode. Figure 1(b) shows the scattered intensities of individual antennas around a wavelength of 730nm, for polarization parallel to the antenna axes. The highest intensity for each column in Fig. 1(b) is indicated by a red circle. Clearly, this maximum does not

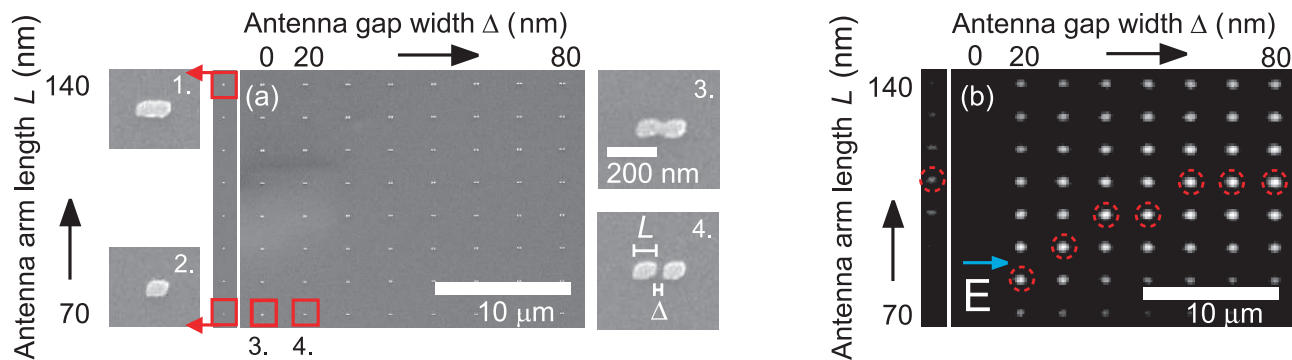


FIG. 1: (color online) (a) SEM image of a nanoantenna array with varied antenna arm lengths (vertical) and antenna gaps (horizontal), with detailed images of several single nanorods and dimer antennas. (b) Scattered intensity detected in a bandwidth of $730 \text{ nm} \pm 30 \text{ nm}$ for polarizations parallel to the antenna long axes. (Circles, red) denote antennas with maximum scattering intensity for each of the columns with constant Δ .

occur for the antennas with the largest particle size, indicating a resonance in the scattering cross section. For small gap widths $\Delta < 50 \text{ nm}$, the maximum shifts to smaller arm lengths L . Antennas with arms that are overlapping, i.e. $\Delta = 0 \text{ nm}$, do not scatter light at the selected wavelength.^{19,20}

A more detailed investigation was made by measuring the spectrally resolved scattered intensity of individual nanoantennas, using a spectrometer equipped with a high-sensitivity CCD camera. Single-antenna spectra were integrated over 30 s and corrected for a background. To increase the signal quality, spectral channels were summed over a bandwidth of 5 nm. Figure 2 shows the resulting scattering spectra of single nanorods with various lengths L of 90 nm (a) and 70 nm (b), for polarization parallel (circles) and perpendicular (diamonds) to the antenna long axis. The two polarizations yield two different resonances corresponding to longitudinal and transverse modes of the nanorods. For the nearly square $70 \times 60 \text{ nm}^2$ particle, the resonances are nearly degenerate. For nanorods with increasing lengths, the longitudinal mode shifts to longer wavelengths while the transverse resonance is unaffected.

We emphasize at this point the strong resemblance of this spectral shift with that observed for small ellipsoidal particles, i.e. using quasistatic Mie-Gans theory.^{16,21} For an ellipsoid, spectral resonances depend only on aspect ratio combined with the characteristic dielectric response of metals with frequency. In the antenna description however, resonances are purely geometrical^{7,8,9,10,11}, and should exist even for a perfect metal (i.e. $\epsilon = -\infty$).¹² Several of our experimental observations support the second interpretation. Firstly, we do not observe the characteristic blueshift of the transverse resonance with increasing aspect ratio for an ellipsoid.^{17,21} Secondly, with a quality factor of around 7, the observed single-antenna resonances are considerably broader than those of small nanorods where factors up to 25 have been reported.¹⁷ Those were explained by the suppression of radiation damping for rods in the quasistatic regime. Our re-

sults are reproduced by theoretical calculations as discussed below, indicating a substantial increase of radiative damping of the antenna modes.

Effects of arm coupling are investigated in Fig. 2(c). Here we have measured the scattering spectra of a dimer antenna with a gap Δ of 20 nm and arm length L of 70 nm. Compared to the isolated rod, the longitudinal mode is redshifted by approximately 50 nm, and is considerably broadened by $\sim 50\%$. Some particle-to-particle variations have been found, which we relate to small deviations in particle shape.^{9,22} Figure 4(a) shows the spectral positions of the longitudinal and transverse modes against L for single nanorods (circles, diamonds) and for coupled dimer antennas (triangles, open squares).

Earlier experimental work on dimers has focused on cylindrical and elliptical particles with fixed aspect ratio.^{19,23,24} The spectral redshift of interacting particles in general is well understood and can be described in terms of plasmon hybridization.²⁵ In contrast to cylinders^{23,26}, we do not observe a blueshift of the transverse antenna mode due to capacitive coupling. The regime of strong interaction for antennas supporting geometrical resonances has been treated only theoretically.¹¹ The redshift of the longitudinal mode dependence on L as a whole in Fig. 4(a) is in good agreement with these calculations. To our knowledge, the associated strong resonance broadening has not been addressed before, as ensemble experiments do not give access to the homogeneous resonance width. We interpret the broadening by superradiance of the coupled antenna arms.²⁵

To validate our experiments, plasmonic modes of dimer nanoantennas are calculated using a scattering formalism based on Green's theorem surface integral equations in parametric form. For a rectangular parallelepiped illuminated along one of its principle axes, the induced components of the electric field are mostly located in the plane perpendicular to this axis along the polarization direction. Therefore, a rectangular rod can be approximated by a two-dimensional calculation.¹² The corresponding 2D-geometries are a $20 \times 60 \text{ nm}^2$ rectangular

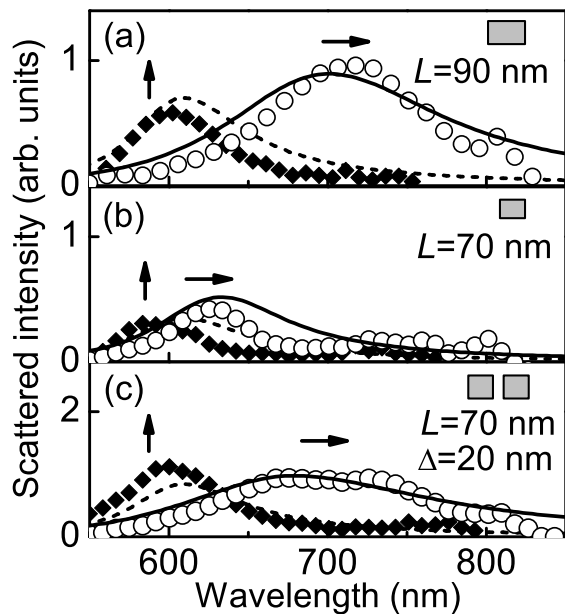


FIG. 2: Experimental scattering spectra of individual gold nanorods with lengths of (a) 90 nm and (b) 70 nm for polarizations parallel (circles) and perpendicular (diamonds) to the nanorod long axis. (c) Same for a dimer nanoantenna with an antenna gap Δ of 20 nm and arm length L of 70 nm. (Lines) Numerical calculations of scattering cross section for transverse (dashed line) and longitudinal (full line) modes.

slab for the transverse resonance, and a $20 \times L$ nm² rectangular slab for the longitudinal resonance. In both cases we assume incidence normal to the long axis of the effective 2D rectangle, with an electric field along the long axis. The lines in Figs. 2(a-c) show the calculated scattering cross sections for the two cases corresponding to transverse (dashed lines) and longitudinal (full lines) polarizations. The calculated resonance positions for different particle lengths are indicated by the lines in Fig. 4(a). Note that in the calculations all the parameters are fixed; reasonably good agreement is obtained without fitting.

A more extensive calculation has been done for all combinations of L and Δ of Fig. 1. Figure 4(b) shows the resulting longitudinal resonance positions. Additionally, the red circles represent combinations (L, Δ) extracted from Fig. 1(b) for which an intensity maximum occurs at $\lambda = 730$ nm [using a fitted L]. The points follow well the calculated contour at $\lambda = 730$ nm, indicated by the red line. We also show results taken at $\lambda = 660$ nm (black squares). Figure 4(b) predicts well the spectral resonance positions in a broad range of antenna parameters. Clearly many combinations of L and Δ result in the same spectral mode position. However, the near-field mode profile will depend strongly on the dimensions of the antenna gap.^{11,12,18}

The calculations provide, next to the scattering cross-sections, also the optical near-fields and the far-field radiation pattern of the antenna. Figure 3(a) shows these

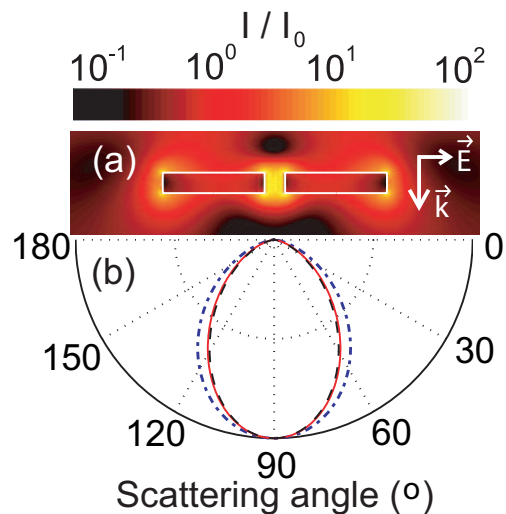


FIG. 3: (color online) (a) Near field intensity at the longitudinal resonance for an antenna with strongly coupled arms ($\Delta = 20$ nm, $L = 100$ nm). (b) Far-field scattering pattern of the antenna (solid line, red), together with the emission patterns of a point dipole (dash-dotted line, blue), and a half-wave antenna (dashed line, black).

for a strongly coupled antenna ($\Delta = 20$ nm, $L = 100$ nm) at resonance, for an incident plane wave as indicated in the figure. The near-field enhancement (shown on a logarithmic scale) reaches 10^2 in the center of the antenna gap. Inside the antenna, the intensity drops to zero at the longitudinal edges of the arms, which is indicative of a half-wave resonance; a quasistatic mode would show a constant internal field. Further evidence is obtained from the corresponding far-field emission pattern, shown in Fig. 3(b) (thick line, red). For comparison we plotted radiation patterns of a point dipole (dash-dotted line, blue), and a half-wave antenna (dashed line, black). Clearly, the antenna pattern corresponds to that of a half-wave dipole antenna, which has a more directional emission than a point dipole due to interference of the radiation emitted over the total antenna length.

In conclusion, we have studied both experimentally and theoretically the scattering of single plasmonic nanoantennas. Darkfield spectroscopy showed a clear dependence of the longitudinal mode on antenna arm length and on gap width for dimers. The absence of a blueshift of the transverse mode indicates the invalidity of the quasistatic ellipsoidal model description. The observation of broad resonances raises the question whether dimer antennas are indeed optimal for nonlinear spectroscopy, as proposed in several papers.^{11,12} In principle enhancements of many orders of magnitude are realizable using both spatial and temporal energy concentration in small particle chains in the quasistatic limit.²⁷ The merit of the dimer antennas may however not be in their temporal energy storage, but in their large size and concomitantly large resonant extinction cross section, coupling effectively more light from a diffraction limited spot into a

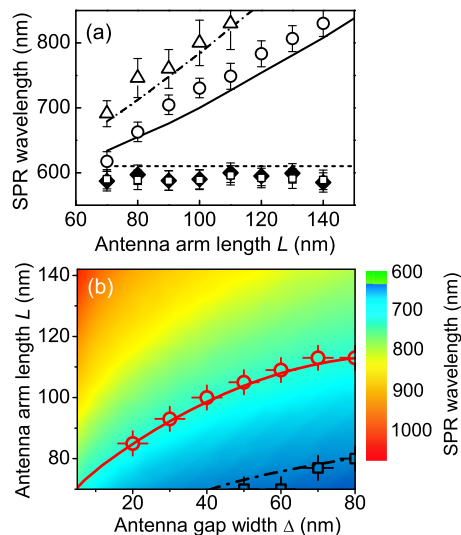


FIG. 4: (Color online) (a) Surface plasmon resonance wavelengths for single nanorods (circles, diamonds) and for dimer antennas with a gap Δ of 20 nm (triangles, open squares), respectively for longitudinal and transverse polarizations. Lines denote resonance positions taken from numerical calculations. (b) Color density graph of calculated longitudinal antenna mode positions, with (line, red) calculated isowavelength contour at $\lambda = 730$ nm. (\square and dashed line, black) same for $\lambda = 660$ nm.

near-field volume.¹³ Additionally, strong radiative damping results in suppression of ohmic losses, which in combination with the strong spatial mode confinement in the antenna gap may be extremely suitable for spontaneous emission enhancement from emitters.¹⁸

We acknowledge B. Ketelaars and P. Vergeer for technical assistance and J. Aizpurua, O. Janssen, H. P. Urbach, W. Vos, H. Mertens, and A. Polman for stimulating discussions. V. G. and J. A. S.-G. acknowledge partial support from the Spanish "Ministerio de Educación y Ciencia" (Grants FIS2006-07894 and FIS2004-0108) and "Comunidad de Madrid" through the MICROSERES network (Grant S-0505/TIC-0191) and V.G.'s PhD scholarship. This work was supported by the Netherlands Foundation "Fundamenteel Onderzoek der Materie (FOM)" and the "Nederlandse Organisatie voor Wetenschappelijk Onderzoek (NWO)," and is part of an industrial partnership program between Philips and FOM.

* Electronic address: muskens@amolf.nl

- ¹ U. Kreibig and M. Volmer, *Optical Properties of Metal Clusters*, Springer Series in Material Science Vol. 25 (Springer-Verlag, Berlin, 1995).
- ² D. Boyer, P. Tamarat, A. Maali, B. Lounis, and M. Orrit, *Science* **297**, 1160 (2002).
- ³ A. D. McFarland and R. P. van Duyne, *Nano Lett.* **3**, 1057 (2003).
- ⁴ W. L. Barnes, A. Dereux, and T. W. Ebbesen, *Nature* **424**, 824 (2003).
- ⁵ T. A. Kelf, Y. Sugawara, J. J. Baumberg, M. Abdelsalam, and P. N. Bartlett, *Phys. Rev. Lett.* **95**, 116802 (2005).
- ⁶ E. Ozbay, *Science* **311**, 189 (2006).
- ⁷ J.-C. Weeber, A. Dereux, C. Girard, J. R. Krenn, and J.-P. Goudonnet, *Phys. Rev. B* **60**, 9061 (1999).
- ⁸ J. R. Krenn, G. Schider, W. Rechberger, B. Lamprecht, A. Leitner, F. R. Aussenegg, and J. C. Weeber, *Appl. Phys. Lett.* **77**(12), 3379 (2000).
- ⁹ H. Ditlbacher, A. Hohenau, D. Wagner, U. Kreibig, M. Rogers, F. Hofer, F.R. Aussenegg, J.R. Krenn, *Phys. Rev. Lett.* **95**, 257403 (2005)
- ¹⁰ K. Imura, T. Nagahara, and H. Okamoto, *J. Phys. Chem. B* **108** 16344 (2004).
- ¹¹ J. Aizpurua, G. W. Bryant, L. J. Richter, F. J. García de Abajo, B. K. Kelley, and T. Mallouk, *Phys. Rev. B* **71**, 235420 (2005).
- ¹² P. Mühlischlegel, H.-J. Eisler, O. J. F. Martin, B. Hecht, and D. W. Pohl, *Science* **308**, 1607 (2005).
- ¹³ P. J. Schuck, D. P. Fromm, A. Sundaramurthy, G. S. Kino, and W. E. Moerner, *Phys. Rev. Lett.* **94**, 017402 (2005).
- ¹⁴ J. N. Farahani, D. W. Pohl, H.-J. Eisler, and B. Hecht,

- Phys. Rev. Lett.* **95**, 017402 (2005).
- ¹⁵ T. Taminiau, R. J. Moerland, F. B. Segerink, L. Kuipers, and N. F. van Hulst, *Nano Lett.* **7**, 28 (2007).
- ¹⁶ S. Link and M. A. El-Sayed, *J. Phys. Chem. B* **103**, 8410 (1999).
- ¹⁷ C. Sönnichsen, T. Franzl, T. Wilk, G. von Plessen, J. Feldmann, O. Wilson, and P. Mulvaney, *Phys. Rev. Lett.* **88**, 077402 (2002).
- ¹⁸ O. L. Muskens, V. Giannini, J. A. Sánchez Gil, and J. Gómez Rivas, to be published.
- ¹⁹ T. Atay, J.-H. Song, and A. V. Nurmikko, *Nano Lett.* **4**, 1627 (2004).
- ²⁰ I. Romero, J. Aizpurua, G. W. Bryant, and F. J. García de Abajo, *Opt. Express* **14** 9988 (2006).
- ²¹ C. F. Bohren and D. R. Huffman, *Absorption and scattering of light by small particles*, 1st ed.; Wiley-VCH: Weinheim, 141-148 (1998).
- ²²
- ²³ W. Rechberger, A. Hohenau, A. Leitner, J. R. Krenn, B. Lamprecht, and F. R. Aussenegg, *Opt. Comm.* **220**, 137 (2003).
- ²⁴ K.-H. Su, Q.-H. Wei, X. Zhang, J. J. Mock, D. R. Smith, and S. Schultz, *Nano Lett.* **3**, 1087 (2003).
- ²⁵ P. Nordlander, C. Oubre, E. Prodan, K. Li, and M.I. Stockman, *Nano Lett.* **4**, 899 (2005).
- ²⁶ J. P. Kottmann and O. J. F. Martin, *Opt. Lett.* **26**, 1096 (2001).
- ²⁷ K. Li, M. I. Stockman, and D. J. Bergman, *Phys. Rev. Lett.* **91**, 227402 (2003).